ResearchGate

See discussions, stats, and author profiles for this publication at: https://www.researchgate.net/publication/51642042

Crystal structure of Arabidopsis thaliana 12-oxophytodienoate reductase isoform 3 in complex with 8-iso prostaglandin A 1

ARTICLE *in* PROTEINS STRUCTURE FUNCTION AND BIOINFORMATICS · NOVEMBER 2011

Impact Factor: 2.63 · DOI: 10.1002/prot.23153 · Source: PubMed

READS

20

7 AUTHORS, INCLUDING:

Byung Woo Han

Seoul National University

55 PUBLICATIONS **393** CITATIONS

SEE PROFILE

Craig A Bingman

University of Wisconsin–Madison

103 PUBLICATIONS **1,604** CITATIONS

SEE PROFILE

Brian G Fox

University of Wisconsin–Madison

212 PUBLICATIONS **7,137** CITATIONS

SEE PROFILE

George N Phillips

Rice University

313 PUBLICATIONS **12,712** CITATIONS

SEE PROFILE

Available from: George N Phillips

Retrieved on: 12 January 2016

NIH Public Access
Author Manuscript
Proteins. Author manuscript; available in PMC 2012 November 1.

Published in final edited form as:
Proteins. 2011 November ; 79(11): 3236–3241. doi:10.1002/prot.23153.

Crystal structure of *Arabidopsis thaliana* 12-oxophytodienoate reductase isoform 3 in complex with 8-*iso* prostaglandin A_1

Byung Woo Han[1,†,*], **Thomas E. Malone**[2,*], **Do Jin Kim**[3], **Craig A. Bingman**[4], **Hyun-Jung Kim**[5], **Brian G. Fox**[4,†], and **George N. Phillips Jr.**[4,†]

[1]Research Institute of Pharmaceutical Sciences, College of Pharmacy, Seoul National University, Seoul 151-742, Korea

[2]Molecular and Environmental Toxicology Program, University of Wisconsin-Madison, Madison, Wisconsin 53706, USA

[3]Department of Chemistry, College of Natural Sciences, Seoul National University, Seoul 151-742, Korea

[4]Department of Biochemistry, Center for Eukaryotic Structural Genomics, University of Wisconsin-Madison, Madison, Wisconsin 53706, USA

[5]College of Pharmacy, Chung-Ang University, Seoul 156-756, Korea

Abstract

12-Oxophytodienoate reductase 3 (OPR3), one of the enzymes involved in the biosynthesis of the plant hormone jasmonic acid (JA), catalyzes the reduction of the cyclopentenone ring of (9*S*, 13*S*)-12-oxophytodienoate [(9*S*,13*S*)-OPDA]. However, there has been no structural information about the interaction between OPRs and the physiologically relevant (9*S*,13*S*)-OPDA. Here we report the crystal structure of *Arabidopsis thaliana* OPR3 in complex with 8-*iso* prostaglandin A1 (8-*iso* PGA_1) which has the same stereochemistry in the cyclopentenone ring as in the physiologically relevant 9*S*,13*S*-OPDA. This structure reveals a new binding mode for substrate that likely contributes to the relaxed stereospecificity observed for AtOPR3.

Keywords

12-oxophytodienoate reductase isoform 3; 8-*iso* prostaglandin A_1; jasmonic acid pathway; *Arabidopsis thaliana*

INTRODUCTION

Jasmonic acid (JA) is a plant secondary messenger that contributes to coordinated responses to many biotic and abiotic stresses, as well as other diverse processes such as pollen maturation and wound responses.[1–2] Biosynthesis of JA originates from linolenic acid in chloroplast membranes, and a number of enzymes are involved in the conversion of this polyunsaturated fatty acid into cyclopentane containing compound JA.[3] 12-oxophytodienoate reductase 3 (OPR3), one of the enzymes involved in the biosynthesis of JA, uniquely catalyzes the reduction of the cyclopentenone ring of (9*S*,13*S*)-12-

[†]Correspondence to: George N. Phillips, Jr., Department of Biochemistry, University of Wisconsin-Madison, 433 Babcock Drive, Madison, WI 53706-1544, USA. phillips@biochem.wisc.edu (or) Brian G. Fox, Department of Biochemistry, University of Wisconsin-Madison, 433 Babcock Drive, Madison, WI 53706-1544, USA bgfox@biochem.wisc.edu (or) Byung Woo Han, College of Pharmacy, Seoul National University, Seoul 151-742, Korea. bwhan@snu.ac.kr.
[*]Byung Woo Han and Thomas E. Malone contributed equally to this work.

NIH-PA Author Manuscript
NIH-PA Author Manuscript
NIH-PA Author Manuscript

NIH-PA Author Manuscript

NIH-PA Author Manuscript

NIH-PA Author Manuscript

oxophytodienoate [(9*S*,13*S*)-OPDA].[4] The JA-deficient phenotype of OPR3 loss-of-function mutants in *Arabidopsis thaliana* indicates that other OPR isoforms cannot substitute for OPR3 in JA biosynthesis.[5]

The physiologically relevant (9*S*,13*S*)-enantiomer of OPDA is not a substrate for the majority of OPRs.[4] Thus the unique function of OPR3 in the biosynthesis of JA is a result of its relaxed stereoselectivity with respect to OPDA stereoisomers. While *Arabidopsis thaliana* OPR3 (AtOPR3) and *Lycopersicon esculentum* OPR3 (LeOPR3) reduce all four stereoisomers of OPDA, the large majority of OPR isoforms seem to resemble LeOPR1 and AtOPR1/2 in their substrate specificity.[6–7] The biological roles of OPR1 and OPR2 have not been established, however, these enzymes efficiently reduce 9R,13R-OPDA but fail to react with the enantiomeric JA precursor 9S,13S-OPDA.[7–9]

To date, the several ligand- and cofactor-bound structures of OPR1 and OPR3 have been reported.[7,10–13] However, there has been no structural information about the interaction between OPRs and the physiologically relevant (9*S*,13*S*)-OPDA. Here we report the crystal structure of AtOPR3 in complex with 8-iso prostaglandin A1 (8-*iso* PGA_1) which has the same α,β-unsaturated carbonyl group and stereochemistry in the cyclopentenone ring as in the physiologically relevant 9*S*,13*S*-OPDA. Our structure shows that hydrogen bonds and van der Waals' interactions between AtOPR3 and 8-*iso* PGA_1 stabilize the substrate molecule for reduction of the alkenyl group within the cyclopentenone ring. The positioning of 8-*iso* PGA_1 reveals a new binding orientation for substrate in the active site that likely contributes to the relaxed stereospecificity observed for AtOPR3 relative to other OPR's.

MATERIALS AND METHODS

Cloning, protein expression, purification, and crystallization

Cloning, expression, purification and crystallization of AtOPR3[12] were as previously described. The calculated molar absorptivity was 43320 M^{-1} cm^{-1}. 8-*iso* PGA_1 was from Cayman Chemical (Ann Arbor, MI). HPLC grade methanol and NADPH were from Sigma-Aldrich (St. Louis, MO).

X-ray data collection, structure determination, and model evaluation

X-ray diffraction data were collected using synchrotron beam line 23-ID at the Advanced Photon Source at the Argonne National Laboratory GM/CA-CAT. The diffraction images were integrated and scaled using HKL2000.[14] The structure of the 8-*iso* PGA_1 bound AtOPR3 was determined by molecular replacement using AtOPR3 structure in complex with FMN (PDB 1q45) as a template. Cross-rotational search followed by translational search was performed utilizing the program using MolRep from CCP4.[15] Subsequent manual model building and refinement were carried out using Coot and Refmac from CCP4 program suite.[15] The stereochemical quality of the refined model was assessed using MolProbity.[16] Structure figures were generated using PyMOL (DeLano Scientific LLC).

Sedimentation equilibrium studies

Sedimentation equilibrium studies were performed with a Beckman Optima XL-A analytical ultracentrifuge in the Biophysics Instrumentation Facility at the University of Wisconsin-Madison. AtOPR1 was dissolved in 5 mM Tris-Hcl at pH 8, containing 50 mM NaCl, while AtOPR3 was dissolved in 5 mM MES-NaOH at pH 6, containing 50 mM NaCl. From a single stock of each protein, dilutions were made to obtain three samples with UV absorbance readings of 0.2 (4.6 μM), 0.5 (11.5 μM) and 0.8 (18.5 μM) at 280 nm. Solvent densities measured using an Anton Paar DMA5000 at 4°C were 1.00241 and 1.00257 g mL^{-1}, respectively. The partial specific volumes for AtOPR1 and AtOPR3 based on their

NIH-PA Author Manuscript

NIH-PA Author Manuscript

NIH-PA Author Manuscript

sequences, neglecting contributions from flavin, were the same, 0.732 mL g^{-1}. For each protein, ~100 μL of each of the three dilutions were placed in 1.2 cm pathlength double-sector, charcoal-filled, epon centerpieces with the appropriate buffers as references. Samples were spun to equilibrium at various speeds at 4°C. Superimposed gradients recorded at 278 nm 2–3 h apart were taken to indicate equilibrium. Data were collected at 278 nm and in most cases at 461 nm and/or 378 nm. A high-speed depletion of protein material from the cells was used as a measure of non-sedimented baseline material. For a given protein, data from all speeds and/or wavelengths were fit to various models including a fixed contribution from the non-sedimented material.

Enzyme reaction

Reactions of AtOPR1, AtOPR2 and AtOPR3 with 8-*iso* PGA_1 and NADPH were monitored by optical spectrometry. A blank was obtained with buffer containing NADPH (150 μM), substrate was added, and the reaction was initiated by addition of enzyme (~1 μM). The oxidation of NADPH resulted in a decrease in absorbance around 340 nm, while reduction of the substrate caused a decrease in the absorption band at ~220 nm. Substrate and product were separated using a Shimadzu VP Series HPLC equipped with a photodiode array spectrophotometer and an ACE C18 column (100 × 4.6 mm, 3 micron particle size) using 70% methanol and 30% water (70:30 v/v) pumped isocratically at 1 mL/min. The substrate and product were monitored and quantified using UV absorption at 218 nm (8-*iso* PGA_1, ε_{218} = 8200 M^{-1} cm^{-1}) and 220 nm (reduced product, ε_{220} = 1700 M^{-1} cm^{-1}).

The masses of 8-*iso* PGA_1 and the reduced product were determined using a Shimadzu LCMS-2010 with an HPLC inlet, an electrospray ionizer, and a quadrupole analyzer at the Paul Bender Chemical Instrument Center at the Department of Chemistry, University of Wisconsin-Madison.

Data deposition

Atomic coordinates and structure factors have been deposited in the RCSB Protein Data Bank (accession code 2G5W).

RESULTS AND DISCUSSION

In order to study the molecular properties that underlie the distinct substrate preferences of OPR3, we analyzed the structure AtOPR3 in complex with 8-*iso* PGA_1 which has the same α,β-unsaturated carbonyl group and stereochemistry in the cyclopentenone ring as in the physiologically relevant (9*S*,13*S*)-OPDA (Fig. 1a and 1b). We soaked the AtOPR3 crystals in a crystallization solution containing 5 mM 8-*iso* PGA_1 and the crystal structure of 8-*iso* PGA_1 bound AtOPR3 was solved to 2.6 Å by molecular replacement using AtOPR3 structure as a phasing model (PDB ID: 1q45).[12] The final model includes two AtOPR3 monomers per asymmetric unit, and each AtOPR3 monomer contains one FMN and one 8-*iso* PGA_1 molecule. The *R* and R_{free} factors were 20.2% and 26.4%, respectively (Table I). The N-terminal (7 residues in chain A; 8 residues in chain B) and C-terminal regions (3 residues in chain A; 5 residues in chain B) of the protein, as well as the L6 loop region (Try285—Glu301 in chain A; Gly289—Asp299 in chain B) in the crystal have not been included in the refined model. The two chains in the asymmetric unit are highly similar to each other, with r.m.s. deviation of 0.25 Å. When compared with the ligand-free AtOPR3 structure,[12] the structure of 8-*iso* PGA_1 bound AtOPR3 has no significant conformational change (Fig. 1c). The previously suspected substrate binding loop region (residues Ile133 to Tyr150), which corresponds to the Lβ3 substrate-binding loop of OPR1, was found to neither move nor interact with 8-iso PGA_1. Likewise, comparison of the ligand-free and (9*R*, 13*R*)-OPDA-bound LeOPR1[10] showed no significant conformational changes.

NIH-PA Author Manuscript

NIH-PA Author Manuscript

NIH-PA Author Manuscript

The cyclopentenone ring of 8-*iso* PGA_1, which is structurally comparable to the corresponding cyclopentenone ring of OPDA, forms stacking interactions with the isoalloxazine ring of the FMN (Fig. 2a), and its carbonyl oxygen is in close contact with the two catalytic histidine residues His186 and His189 (Fig. 2b). The double bond formed by C10 and C11 carbon atoms of the cyclopentenone ring of the bound 8-*iso*-PGA_1 is located closely to both hydride (FMN-N5) and proton (Tyr191-OH) donors, suggesting that the cyclopentenone ring in 8-*iso*-PGA_1 has been effectively oriented for redox chemistry in this enzyme-substrate complex (Fig. 2a). While the gatekeeper residues Tyr78 and Tyr246 of AtOPR1 form a narrow entrance into the cavity above the FMN, the corresponding amino acids of AtOPR3, Phe74 and His245, turn away from the active site, giving rise to a widening of the cavity in OPR3 (Fig. 2b). The importance of this position in stereoselectivity is also supported by substitution of the corresponding phenylalanine and histidine residues in LeOPR3 with tyrosine residues, which shifted the specificity of the mutated enzymes toward (9*R*,13*R*)-OPDA over (9*S*,13*S*)-OPDA.[13] These geometrical differences most likely account for the high degree of substrate stereoselectivity of OPR1 and the more relaxed specificity of OPR3 as proposed earlier.[13]

Compared to (9*R*,13*R*)-OPDA bound to LeOPR1,[10] the binding mode of the cyclopentenone ring of 8-*iso*-PGA_1 differs in the distance of the double bond and its angle relative to FMN-N5 (Fig. 2a). The small differences in the positions of the cyclopentenone rings propagate into much larger differences in the positions of the alkyl chains as they emerge from the interior of the active site (Fig. 2b). These discrepancies imply that contacts of the alkyl chains with distal residues may have important contributions to the differences in substrate specificity observed for OPR isoforms. As a result, the 8*S* tail of 8-*iso*-PGA_1 has van der Waals interactions with the side chains of His189 and Ile243 (Fig. 2b). These interactions potentially mimic hydrophobic interactions with the 13*S* pentenyl side chain of the natural substrate. The methyl end of the 12*S* tail of the bound 8-*iso*-PGA_1 locates within 4 Å of the aliphatic part of the Arg367 side chain and within 6 Å of the guanidinium group. Since the methyl group of the 12*S* tail of 8-*iso*-PGA_1 is replaced by a carboxyl group in the natural substrate (9*S*,13*S*)-OPDA, (Fig. 2b), a hydrogen bonding interaction between the natural substrate and the guanidinium group of Arg367 may stabilize the natural substrate-enzyme complex. In addition, the strong hydrogen bond between the PGA1 carboxyl group and the main chain nitrogen of Arg284 that might pull the substrate more out of the cavity than (9S, 13S)-OPDA and that leads to very weak hydrogen bonds of the carbonyl oxygen to the two activating histidines.

In order to confirm that 8-*iso*-PGA_1 was an effective substrate for AtOPR3, we performed an enzymatic assay using 8-*iso*-PGA_1 as a substrate (Fig. 2c). The result indicated that 8-*iso*-PGA_1 was an active substrate for AtOPR3 with apparent k_{cat} and K_M values of 0.23 s^{-1} and 22 μM, respectively. Of the three *Arabidopsis* OPR isoforms tested, only AtOPR3 reduced 8-*iso*-PGA_1, while AtOPR1 and AtOPR2 did not (Fig. 2c). This result is consistent with the stereochemical preferences previously established for the JA pathway and with the known reactions of the AtOPR isoforms with the different OPDA stereoisomers.[17]

While most OPRs have been described as monomers, LeOPR crystallizes as a self-inhibited dimer, in which the substrate binding pocket is occupied by loop L6 of the neighboring protomer.[7,13] In contrast to the self-inhibited dimeric structure of LeOPR3, the structure of substrate-free and 8-*iso*-PGA_1-bound structures of OPR3 showed that the protein exists as a monomer in the crystal. Incorporation of 8-*iso*-PGA_1 into the active site was not affected by crystal packing while soaking the OPDA substrate into LeOPR3 crystals or cocrystallization trials were unsuccessful. Furthermore, sedimentation equilibrium measurements on AtOPR1 and AtOPR3 showed that both proteins were monomers at concentrations up to ~30 μM, at which LeOPR3 forms a self-inhibited dimer (Fig. 2d).[13]

NIH-PA Author Manuscript

NIH-PA Author Manuscript

NIH-PA Author Manuscript

In the crystal structure of LeOPR3, the sulfate is located at the dimer interface, close to Tyr364, and is positioned perfectly to mimic a phosphorylated tyrosine residue.[7] The bound sulfate ion directly interacts with the protruding loop L6 from the protomer, stabilizing the dimer formation of the protein. Thus, it has been suggested that dimerization and hence OPR3 activity may be regulated by the reversible phosphorylation of Tyr364 in vivo.[7] In the structures of substrate-free and 8-*iso*-PGA_1 bound AtOPR3 the two monomers observed in the asymmetric unit of AtOPR3 crystals can be superimposed with the corresponding protomers of the LeOPR3 dimer, suggesting a similar dimeric structure for AtOPR3. Although the L6 loop of AtOPR3 is poorly defined in the refined structure, it clearly protrudes toward the active site of the molecular neighbor in a similar fashion as in LeOPR3. Considering that the amino acid sequence of the loop L6 is highly conserved among the OPR3-like enzymes, it is still intriguing that OPR3 activity is regulated by self-inhibitory dimerization, which might be controlled by reversible phosphorylation of the protein, although it awaits further characterizations to confirm this hypothesis.

Acknowledgments

Grant sponsor: NIH; Grant number: GM064598, GM074901 (Protein Structure Initiative), and T32 GM08349 (Institutional Biotechnology Pre-Doctoral Training Grant);

Grant sponsor: NSF; Grant number: MCB-0316232;

Grant Sponsor: Korea Ministry of Education, Science and Technology; Grant number: 2011-0004305, 2011-0027449, and NRF-M1AXA002-2010-0029770 (Basic Science Research Program and the Global Frontier through the National Research Foundation);

Grant sponsor: Korea Ministry of Health and Welfare (Korea Healthcare Technology R&D Project); Grant number: A092006;

Grant sponsor: Seoul National University (Research Settlement Fund for the new faculty).

The authors thank all members of the Center for Eukaryotic Structural Genomics for various important contributions. Beamline 23-ID at the Argonne National Laboratory GM/CA-CAT is supported by the National Cancer Institute (Y1-CO-1020) and the National Institute of General Medical Science (Y1-GM-1104). The Advanced Photon Source is supported by the U.S. Department of Energy, Basic Energy Sciences.

Abbreviations

OPR3	12-oxophytodienoate reductase isoform 3
PGA_1	prostaglandin A1
JA	jasmonic acid

References

1. Liechti R, Farmer EE. The jasmonate pathway. Science. 2002; 296(5573):1649–1650. [PubMed: 12040182]
2. Strassner J, Schaller F, Frick UB, Howe GA, Weiler EW, Amrhein N, Macheroux P, Schaller A. Characterization and cDNA-microarray expression analysis of 12-oxophytodienoate reductases reveals differential roles for octadecanoid biosynthesis in the local versus the systemic wound response. Plant J. 2002; 32(4):585–601. [PubMed: 12445129]
3. Vick BA, Zimmermann DC. Distribution of a Fatty Acid cyclase enzyme system in plants. Plant Physiol. 1979; 64(2):203–205. [PubMed: 16660932]
4. Schaller A, Stintzi A. Enzymes in jasmonate biosynthesis - structure, function, regulation. Phytochemistry. 2009; 70(13–14):1532–1538. [PubMed: 19703696]

NIH-PA Author Manuscript

NIH-PA Author Manuscript

NIH-PA Author Manuscript

5. Stintzi A, Browse J. The Arabidopsis male-sterile mutant, opr3, lacks the 12-oxophytodienoic acid reductase required for jasmonate synthesis. Proc Natl Acad Sci U S A. 2000; 97(19):10625–10630. [PubMed: 10973494]
6. Schaller F, Biesgen C, Mussig C, Altmann T, Weiler EW. 12-Oxophytodienoate reductase 3 (OPR3) is the isoenzyme involved in jasmonate biosynthesis. Planta. 2000; 210(6):979–984. [PubMed: 10872231]
7. Breithaupt C, Kurzbauer R, Lilie H, Schaller A, Strassner J, Huber R, Macheroux P, Clausen T. Crystal structure of 12-oxophytodienoate reductase 3 from tomato: self-inhibition by dimerization. Proceedings of the National Academy of Sciences of the United States of America. 2006; 103(39): 14337–14342. [PubMed: 16983071]
8. Schaller F, Hennig P, Weiler EW. 12-Oxophytodienoate-10,11-reductase: occurrence of two isoenzymes of different specificity against stereoisomers of 12-oxophytodienoic acid. Plant physiology. 1998; 118(4):1345–1351. [PubMed: 9847108]
9. Biesgen C, Weiler EW. Structure and regulation of OPR1 and OPR2, two closely related genes encoding 12-oxophytodienoic acid-10,11-reductases from Arabidopsis thaliana. Planta. 1999; 208(2):155–165. [PubMed: 10333582]
10. Breithaupt C, Strassner J, Breitinger U, Huber R, Macheroux P, Schaller A, Clausen T. X-ray structure of 12-oxophytodienoate reductase 1 provides structural insight into substrate binding and specificity within the family of OYE. Structure. 2001; 9(5):419–429. [PubMed: 11377202]
11. Fox BG, Malone TE, Johnson KA, Madson SE, Aceti D, Bingman CA, Blommel PG, Buchan B, Burns B, Cao J, Cornilescu C, Doreleijers J, Ellefson J, Frederick R, Geetha H, Hruby D, Jeon WB, Kimball T, Kunert J, Markley JL, Newman C, Olson A, Peterson FC, Phillips GN Jr, Primm J, Ramirez B, Rosenberg NS, Runnels M, Seder K, Shaw J, Smith DW, Sreenath H, Song J, Sussman MR, Thao S, Troestler D, Tyler E, Tyler R, Ulrich E, Vinarov D, Vojtik F, Volkman BF, Wesenberg G, Wrobel RL, Zhang J, Zhao Q, Zolnai Z. X-ray structure of Arabidopsis At1g77680, 12-oxophytodienoate reductase isoform 1. Proteins. 2005; 61(1):206–208. [PubMed: 16080145]
12. Malone TE, Madson SE, Wrobel RL, Jeon WB, Rosenberg NS, Johnson KA, Bingman CA, Smith DW, Phillips GN Jr, Markley JL, Fox BG. X-ray structure of Arabidopsis At2g06050, 12-oxophytodienoate reductase isoform 3. Proteins. 2005; 58(1):243–245. [PubMed: 15468319]
13. Breithaupt C, Kurzbauer R, Schaller F, Stintzi A, Schaller A, Huber R, Macheroux P, Clausen T. Structural basis of substrate specificity of plant 12-oxophytodienoate reductases. J Mol Biol. 2009; 392(5):1266–1277. [PubMed: 19660473]
14. Otwinowski Z, Minor W. Processing of X-ray diffraction data collected in oscillation mode. Methods Enzymol. 1997; 276:307–326.
15. Murshudov GN, Vagin AA, Dodson EJ. Refinement of macromolecular structures by the maximum-likelihood method. Acta Crystallogr D Biol Crystallogr. 1997; 53:240–255. [PubMed: 15299926]
16. Lovell SC, Davis IW, Arendall WB 3rd, de Bakker PI, Word JM, Prisant MG, Richardson JS, Richardson DC. Structure validation by Calpha geometry: phi,psi and Cbeta deviation. Proteins. 2003; 50(3):437–450. [PubMed: 12557186]
17. Schaller F. Enzymes of the biosynthesis of octadecanoid-derived signalling molecules. J Exp Bot. 2001; 52(354):11–23. [PubMed: 11181709]

NIH-PA Author Manuscript

NIH-PA Author Manuscript

NIH-PA Author Manuscript

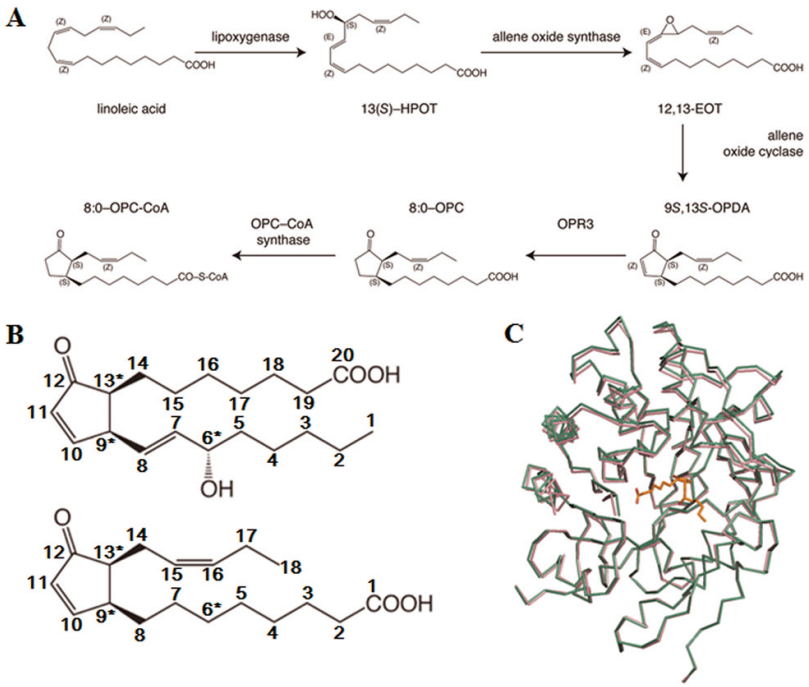

Figure 1.

(A) Schematic representation of jasmonic acid biosynthesis.

(B) Structures of 8-iso-PGA1 (top) and (9S,13S)-OPDA (bottom).

(C) Aligned structures of FMN-bound AtOPR3 (colored in pink) and 8-iso-PGA1-FMN-AtOPR3 complex (colored in green). The bound PGA1 is shown in sticks.

NIH-PA Author Manuscript

NIH-PA Author Manuscript

NIH-PA Author Manuscript

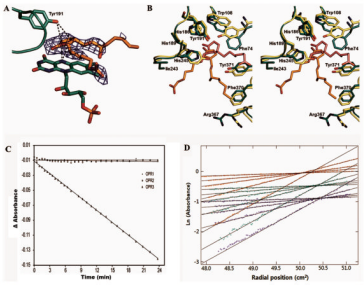

Figure 2.

(A) Orientation of the bound 8-iso-PGA1 relative to the FMN and the general acid Tyr191. The *Fo* − *Fc* electron density of the bound 8-iso-PGA1 is contoured at 2.5 σ. The interactions of the double bond-forming carbon atoms of 8-iso-PGA1 with N5 nitrogen atom of FMN and the general acid Tyr191 are indicated by dotted lines.

(B) Stereo view of the substrate binding site of the 8-iso-PGA1-FMN-AtOPR3 complex structure (green) overlaid with the structure of (9R,13R)-OPDA-FMN-LeOPR1 complex (light green) after structural alignment. Residues are numbered according to the AtOPR3 sequence. The FMN molecules of the enzymes superimpose perfectly with each other and are left out for clarity.

(C) Enzymatic assay results of three *A. thaliana* OPR isoforms using 8-iso-PGA1 as a substrate. Time-dependent change in A340 observed from AtOPR1, AtOPR2, and AtOPR3 are indicated by circles, rectangles, and triangle, respectively.

(D) Sedimentation equilibrium data for three concentrations of AtOPR3 (blue, 4,6 μM; green, 11.5 μM; red, 18.5 μM) and 5 speeds (4.2k, 6.6k, 8.6k, 12k, 17.5k) detected at 278 nm. Global curve fitting was consistent with the presence of a single species at all concentrations observed. The average molecular weight from the global fit of data to the 278 nm data was 44,101 ± 41 Da for AtOPR3. These results are in good agreement with the molecular weight from sequence of 42,694 Da. Data obtained at other wavelengths (378 nm or 461 nm, corresponding to FAD absorption peaks) were consistent with this analysis and their inclusion in global fits minimally impacted the calculated weight average molecular weights.

NIH-PA Author Manuscript

NIH-PA Author Manuscript

NIH-PA Author Manuscript

Table I

Statistics for data collection and model refinement

Data collection[a]	**AtOPR3 in complex with 8-iso PGA_1**
Space group	$P2_12_12_1$
Cell dimensions	
a, b, c (Å)	79.70, 86.61, 123.58
α, β, γ (°)	90, 90, 90
Resolution (Å)[b]	50.00–2.58 (2.67-2.58)
No. reflections	22750
R_{merge} (%)[c]	15.7 (36.6)
I/σI[d]	9.55 (3.42)
Completeness (%)	82 (50)
Redundancy	6.1 (3.9)
Refinement [e,f]	
Resolution (Å)	48.83 - 2.58 (2.64-2.58)
No. reflections	22704 (927)
R_{work} / R_{free}	0.202 / 0.264 (0.290 / 0.430)
No. of atoms	
Protein	5627[g]
Ligand/ion	110[h]
Water	108
Mean B-value (overall)	39.82
Ramachandran analysis	
Most favored regions	273 (89.2%)
Additional allowed regions	33 (10.8%)
Disallowed regions	0 (0%)
R.m.s deviations	
Bond lengths (Å)	0.006
Bond angles (°)	0.977

[a] Data collected at Sector 32 of the Advanced Photon Source.

[b] Numbers in parentheses indicate the highest resolution shell of 20.

[c] $R_{merge} = \Sigma_h \Sigma_i |I(h)_i - \langle I(h) \rangle| / \Sigma_h \Sigma_i I(h)_i$, where $I(h)$ is the observed intensity of relection h, and $\langle I(h) \rangle$ is the average intensity obtained from multiple measurements.

[d] The root-mean-squared value of the intensity measurements divided by their estimated standard deviation.

[e] $R_{work} = \Sigma | |F_O| - |F_C| | / \Sigma |F_O|$, where $|F_O|$ is the observed structure factor amplitude and $|F_C|$ is the calculated structure factor amplitude.

[f] R_{free} = R-factor based on 4.96% of the data excluded from refinement.

[g] Number of non-hydrogen protein atoms included in refinement.

[h] These include FMN and 8-*iso* PGA_1.

NIH-PA Author Manuscript
NIH-PA Author Manuscript
NIH-PA Author Manuscript